

# **Queue profile estimation in signalized arterials by utilizing probe vehicle data**

**Mohsen Ramezani, EPFL-LUTS  
Nikolas Geroliminis, EPFL-LUTS**

**Conference paper STRC 2013**

**STRC**

**13<sup>th</sup> Swiss Transport Research Conference**  
Monte Verità / Ascona, April 24-26, 2013

# Queue profile estimation in signalized arterials by utilizing probe vehicle data

Mohsen Ramezani  
EPFL-ENAC-LUTS  
Lausanne

Nikolas Geroliminis  
EPFL-ENAC-LUTS  
Lausanne

Phone: +41 21 69 32484  
Fax: +41 21 69 35060  
email: mohsen.ramezani@epfl.ch

Phone: +41 21 69 32481  
Fax: +41 21 69 35060  
email: nikolas.geroliminis@epfl.ch

## Abstract

Queues at signalized intersections are one of the main causes of traffic delays and urban traffic state variability. Hence, a method to estimate characteristics of queues provides a better understanding of urban traffic dynamics and also a performance measurement of signalized arterials. In order to capture the evolution of queues, we aim at leveraging the collective effect of spatially and temporally dispersed GPS data to identify the queue profile in the time-space plane that designates the manner of formation and dissipation of queues. The queue profile characterizes the time evolution of both queue front and back, which consequently can be separated in a two-step estimation process resulting to the queue profile polygon. The evolution of queue front, in the time-space diagram, based on the kinematic traffic shockwave theory is modeled as a line with the known slope of queue-discharging shockwave. The evolution of back of queue is more challenging and modeled as a piecewise linear function where slope of segments is between the queue-discharging shockwave and zero. In the proposed method, the input data consists of position and velocity of GPS-equipped probe vehicles. In addition, the queue profile estimation method does not require any explicit information of signal settings and arrival distribution. The proposed method is tested with various penetration rates and sampling intervals of GPS data, which reveals promising results once compared to a uniform arrival queue profile estimation procedure. The proposed method could be beneficial for spillback identification, vehicle trajectory construction, and fuel consumption and emission estimation.

## Keywords

Queue profile estimation – Kinematic traffic shockwave model – GPS-equipped probe vehicles

# 1. Introduction

Presence of vehicle queues at intersections is the crucial cause of variability of drivers' experienced delay in urban networks, which is the principal performance measure of level of service at signalized intersections. Most of the existing models of travel times ignore spatiotemporal correlations among adjacent roads and traditional models estimate average quantities, which cannot capture travel time reliability. Hence, a reliable and practical queue estimation method is of great importance for intelligent transportation systems (ITS) to provide a better understanding of the intersection dynamics, facilitate the estimation of travel time distributions and later solve the traffic signal control problem. Nevertheless, capturing the temporal-spatial characteristics of queue formation and dissipation in urban arterials is still a challenging task. Considering that queue arrivals at intersections are influenced by departures from upstream signals, an assumption of uniform or Poisson arrivals is not valid, especially for short intersections. Therefore, we aim at modeling the evolution of queues by introducing the concept of queue profile that defines the manner of formation and dissipation of queues in the time-space (x-t) plane. Queue profile is a polygon in the x-t plane that its every edge designates a traffic shockwave based on kinematic LWR theory (Lighthill and Whitham, 1955; Richards, 1956). By estimating the queue profile for each cycle, we can derive various performance measures including, number of vehicles in the queue, position of back and front of the queue, and total and average delay per vehicle. In addition, given the queue profile the vehicle trajectories can be reconstructed, which is fundamental for fuel consumption and emission estimation and travel time decomposition problem (Hellinga et al., 2008).

Literature of queue estimation can be theoretically grouped into two modeling classes: i) models based on the cumulative traffic input-output (Webster, 1958; Akcelik, 1998; Viti and van Zuylen, 2010), with the limitation that these models are insufficient to provide the spatial distribution of queue dynamics (Michalopoulos et al., 1981), and ii) models based on LWR shockwave theory (Skabardonis and Geroliminis, 2008; Ban et al., 2011; Wu and Liu, 2011), which provide temporal-spatial dynamics of queuing process requiring perfect input data. Further, many pivotal studies of queue and delay estimation in transportation research (Newell, 1960; Darroch et al. 1964; Newell, 1965; McNeill, 1968) are based (fully or partially) on rather limiting assumptions in order to result in closed-form theoretical solutions. These assumptions can be summarized as: i) known signal setting, ii) known initial queue size at the start of the cycle, iii) known arrival pattern (e.g. uniform, Poisson), and iv) condition that expected value of arrivals do not (constantly) exceed the signal capacity (Dion et al., 2004).

Evidently, signal settings (i.e. cycle length and splits) are not readily available, specifically in case of actuated signals. In addition, a known arrival distribution might be considered valid in case of an isolated intersection, whereas in arterials, this assumption neglects the impact of upstream intersections which alter the arrival pattern at downstream intersections. In this study, the proposed queue profile estimation method attempts to relax the aforementioned assumptions.

Prevailing queue estimation methods employ several monitoring technologies, e.g. loop detectors (Skabardonis and Geroliminis, 2008; Geroliminis and Skabardonis, 2011; Wu et al., 2011), and event-based signal and vehicle data [Wu et al., 2010]. Recently, the emergence and a steadily increase of public deployment of user-based data collection systems, e.g. GPS-equipped vehicles (Herrera et al., 2010) and vehicle re-identification using cellphones or

wireless magnetic sensors (Kwong et al., 2009), provides a great potential for probe vehicles in ITS applications. Kwong et al. (2009) is one of the few efforts to estimate performance measures without the need for signal settings information, but it requires wide deployment of sensors. Ramezani and Geroliminis (2012) develop a methodology based on the link travel times of probe vehicles to estimate the arterial travel time distribution by considering spatial-temporal nonlinear correlations. In (Hofleitner et al., 2012), a probabilistic framework for estimation of arterial traffic state using sparse probe vehicle data is proposed. Comert and Cetin (2011) provide an analytical model for queue length estimation of an isolated intersection with the assumption of Poisson arrival distribution and examined the effect of probe vehicles penetration rate. In addition, in (Izadpanah et al., 2009) a queue estimation method based on the identification of shockwaves from probe vehicle trajectories is studied. Although queue estimation is straightforward given trajectory of probe vehicles with large penetration rates, for practical purposes with low penetration rate of probe vehicles, advanced techniques that combine optimization and physical properties of the traffic flow seems essential. However, mobile traffic sensors cannot provide occupancy and flow information similar to loop detectors, because their data are samples of true traffic information. This raises challenges since mobile traffic data cannot be readily applied to common queue estimation methods.

This paper is organized as follows. Section 2 presents the preliminaries of the traffic flow modeling that we utilize for the queue profile estimation. In Section 3, we introduce the proposed method and elaborate on its details. In Section 4, the results are presented and compared with a uniform arrival queue estimation procedure, and finally, the paper concludes in Section 5.

## 2. Background

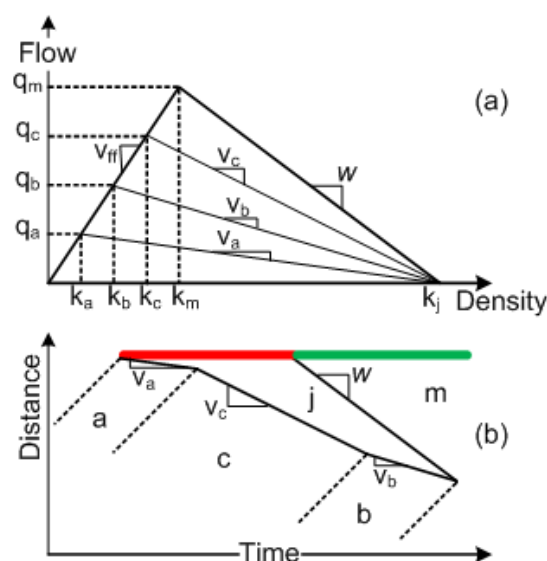
This paper aims at estimating the queue profile that is a polygon in the  $x$ - $t$  plane modeling the formation and dissipation of the queue during signal cycles such that every edge of the queue profile polygon designates a traffic shockwave. Based on LWR theory, shockwaves are boundaries determining flow-density discontinuities in the traffic stream, i.e. points on the border between two different traffic states. Thus, crossing traffic shockwaves, the slope of vehicle trajectory in the  $x$ - $t$  plane (i.e. speed of the vehicle) changes abruptly. In this study, for each link of the urban network we assume a triangular fundamental diagram (FD) characterized by, the maximum flow (capacity,  $q_m$ ), the free flow speed,  $v_{ff}$ , and the jam density,  $k_j$ , see Fig. 1a.

Fig. 1b depicts a queue profile at a signalized intersection comprising the queue discharging shockwave as the representation of front of queue and a 3-segment piecewise linear shockwave as the back of queue. As it is apparent, the queue discharging shockwave separates the traffic state at capacity (denoted by **m**) from the jammed state (denoted by **j**). Likewise, the 3-segment shockwave of the back of queue separates the jammed state from 3 different traffic states (denoted by **a**, **b**, and **c**). The slope of shockwave between traffic states  $s$  and  $s'$  and specifically the slope of queue discharging shockwave are, respectively:

$$v_{ss'} = \frac{q_s - q_{s'}}{k_s - k_{s'}}, w = \frac{q_m}{v_{ff} - k_j}. \quad (1)$$

Note that, the proposed queue profile estimation does not require any arrival pattern information. Therefore, the extent and slope of shockwaves cannot be estimated based on LWR theory. Nevertheless, by estimation of queue profile, the reverse modeling is possible such that the attributes of shockwaves and consequently the characteristics of arrival traffic state can be determined.

Figure 1 The fundamental diagram and a queue profile at a signalized intersection.



In this paper, we try to estimate the queue profile polygon from probe vehicles. Probe vehicles provide samples of their individual traffic state and we aim at leveraging the collective information of temporally and spatially dispersed probe data. As we stated earlier, the speed of vehicles changes when their trajectories cross shockwaves. In urban networks and particularly at signalized intersections, this associates with how probe vehicles join and leave the queue. Hence, it is necessary to investigate the time and position that a probe vehicle joins and leaves the queue. So, the proposed method utilizes the formula of kinematics to approximate the time and the position that a probe vehicle joins and leaves the queue (joining and leaving points) from its reported data by assuming constant acceleration ( $a_{acc}$ ) and deceleration ( $a_{dec}$ ) of vehicles. This assumption is not expected to influence the accuracy of the model (Geroliminis and Skabardonis, 2005).

### 3. Method

In this section, we introduce and elaborate on the principal steps of the proposed queue profile estimation method. Let us assume that probe vehicle  $i$  reports its position (the distance from the beginning of the link,  $x_i^k$ ) and velocity ( $v_i^k$ ) along with the time stamp ( $t_i^k$ ) at time step  $k$  periodically, with sampling interval  $T$  (s). The errors in measurements or map matching are not addressed in this work. Note that the queue profile estimation can be done for each link independently from other links as long as there are no spillbacks. In case spillbacks might occur, the queue profile estimation should be done from downstream to upstream links to capture the spillback blockage development. An example of the queue profile estimation with  $T = 30$  (s) and penetration rate ( $\phi$ ) of 40% is depicted in Fig. 2, where ground truth and estimated queue profiles are respectively denoted by black and red polygons. Note that probe report data points are the input to the method and trajectories are illustrated for better understanding of queue dynamics. Even if this penetration rate is not realistic, it is chosen for illustration purposes. Later, smaller values of  $\phi$  are scrutinized.

An overview of the queue profile estimation method is as follows. Since we do not assume any information of signal settings, we need to identify the stopped data points and assign them to various groups that each group represents a cycle. Therefore in Section 3.1, we classify all of the GPS input data to two groups, stopped and moving, based on the velocity attribute of data. In Fig. 2, red squares denote the stopped data points while black diamonds denote the moving data points. Afterwards in Section 3.2, we introduce a clustering algorithm based on the projection profile algorithm to cluster the stopped data points into different signal cycles. Subsequently, in Section 3.3 the moving data are assigned to different cycles. Fig. 2 depicts the cycle number of each stopped and moving data. It is a well-known fact that the queued vehicles discharge at the capacity flow, which based on LWR theory results to the queue discharging shockwave designated by a line with slope  $w$  in the  $x$ - $t$  diagram. In addition, the leaving points of vehicles from the queue (filled blue points in Fig. 2) are on the queue discharging shockwave. Hence, the estimation of front of queue for each cycle can be formulated as a constrained least square problem, which is presented in Section 3.4. The proposed method does not require the distribution of arrival pattern to estimate queue profiles, thus, we model the back of queue as a piecewise linear function shockwave, that fits to the joining points of vehicles to the queue (filled green, cyan, and yellow points in Fig. 2). In Section 3.5, a curve-fitting nonlinear optimization method is introduced to identify the number and characteristics of the piecewise linear function (Groot et al., 2012). In the sequel, the link index is omitted for simplicity.

#### 3.1 Classification of probe data to moving and stopped groups

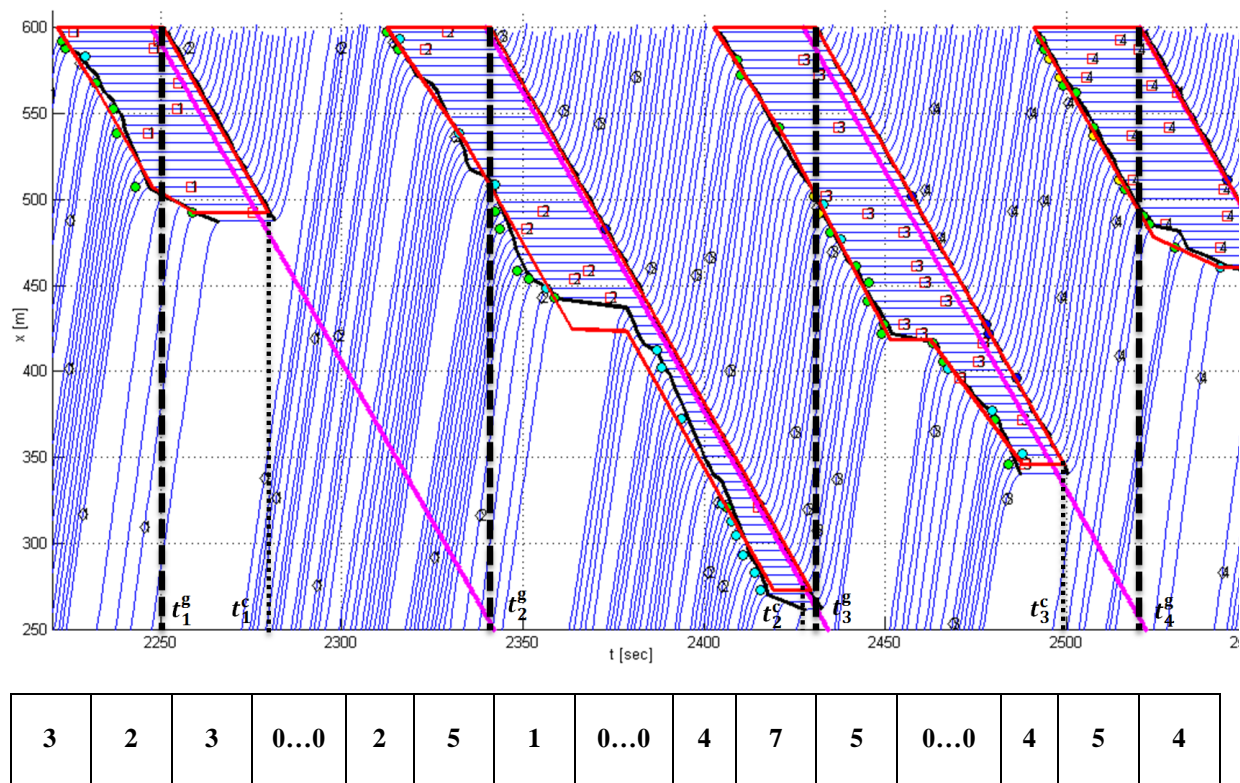
The first step of the procedure is to classify the probe data into two classes of moving and stopped (m, s) to be able to apply the LWR approach. This can be done with a threshold-based classifier:

$$c_i^k = \begin{cases} m & \text{if } v_i^k > v_{th} \\ s & \text{if } v_i^k \leq v_{th}, \end{cases} \quad (2)$$

where  $v_{th}$  (m/s) is a threshold parameter to designates the vehicles with velocity close to zero as stopped.

Though the correct classification rate of the proposed classifier is 100% in case of exact data, errors in velocity measurements degrade the classifier performance, but do not significantly affect the whole methodology. Therefore, an approximate velocity measurement, e.g. utilizing differential GPS or fusion of GPS speed information with vehicle speedometer seems essential, given also that signal settings are considered unknown. The classification of probe data points to stopped (red square) and moving (black diamond) is depicted in Fig. 2.

Figure 2 An illustrative example of the queue profile estimation method. The table is the accumulator projection vector corresponding to Section 3.2.



### 3.2 Clustering the stopped data to cycles

Existing queue estimation methods are applicable for signal cycles and with no information of signal settings, the number and duration of cycles are unknown. Hence, in the second step of the procedure a clustering technique is needed to cluster the stopped data into various groups that each group represents a cycle. By scrutinizing the temporal and spatial distribution of stopped data in the  $x$ - $t$  plane, we notice that the stopped data of two consecutive cycles can be linearly separated with a straight line with slope  $w$  that lies properly between the two groups. Therefore, a clustering technique based on the projection profile method (Jelaca et al., 2012) is proposed to cluster the stopped data into cycles. The purpose of projection profile method is to extract a scalar feature from the dispersed data of stopped vehicles in the  $x$ - $t$  plane. Thus, we introduce a projection function  $\mathcal{P}$  such that projects every *stopped vehicle* data (2-D) along some parallel lines into an accumulator projection vector over the line  $x = 0$  (the entrance of link), where at this location, time is divided to equal

intervals (bins) such that each bin is associated with the number of projected points lying inside the bin. Parallel lines are a set of straight lines all with slope  $w$  (as vehicles depart from the queue at capacity flows) in  $x$ - $t$  plane, which covers the time interval of analysis,

$$\text{if } c_i^k = s \Rightarrow \mathcal{P}(t_i^k, x_i^k) = t_i^k - \left(\frac{x_i^k}{w}\right). \quad (3)$$

One expects that the projection profile method should create i) clusters of adjacent bins with positive values, representing the red interval of a cycle, and ii) clusters of adjacent bins with zero value, representing the green duration of a cycle. Consequently, the stopped data associate with every cluster of stopped bins (adjacent bins with positive value) corresponds to a common cycle. This procedure with values of the accumulator projection vector is illustrated in Fig. 2. The accuracy of projection profile algorithm depends on the bin size ( $s$ ). To determine the size of each bin, one should consider that large values cannot discriminate between cycles and small values may decrease the chance that stopped data points belonging to the same cycle being projected into adjacent bins. (In case of small size bins, the number of bins with zero value during the red interval increases. This might create group of zero bins during the red interval.) We test the sensitivity of the projection profile algorithm to various bin sizes and values between 4 and 10 (s) show acceptable outcomes. In this study, we set the bin size equal to 10 (s). Result of this stage is apparent in Fig. 2, where the cycle number of each stopped data is stated. Note that this method is still valid in case of spillbacks that block departures during green times of upstream intersections. Even if the estimated durations might be different than the exact values of each signal phase (e.g. in case of spillbacks or no arrivals), they will produce an accurate queue profile in the next methodological steps.

### 3.3 Associating the moving vehicles to cycles

Previous step identifies the number of cycles and assigns stopped data to their corresponding red duration. Likewise, the proposed queue profile estimation method needs the moving data to be associated to cycles, to formulate the estimation problem of front and back of queue. Let us assume  $S_j$  denotes the set of stopped data assigned to cycle  $j$ . One can fit a line with slope  $w$  to every data point that belongs to  $S_j$ . The line with the largest intercept can be regarded as a lower envelope of the “true” discharging line, see magenta lines in Fig. 2. This line can be regarded as a linear boundary to distinguish between moving data of every cycle, e.g. the moving data on the left side of this line for cycle  $j$ , and right side of the corresponding line of the cycle  $j - 1$  are considered as the moving data of cycle  $j$ . We denote the set of moving data associate with cycle  $j$  as  $M_j$ . Fig. 2 depicts the number of the cycle that each moving data is assigned to.

### 3.4 Estimation of the front of queue

Fundamentally, queuing process can be divided to two distinct processes, formation and dissipation of the queue, which in urban networks is associated with the traffic signal alteration. The fourth step of the queue profile procedure is to determine the queue dissipation phase for every cycle ( $j$ ). It is a well-known fact that the queued vehicles discharge at the capacity flow, which based on LWR theory results to a shockwave designated by a line with slope  $w$  in the  $x$ - $t$  diagram. Hence, to estimate the front of the queue (discharging line) there is only one parameter, i.e. the line intercept, to be determined. This line will separate stopped

from moving vehicles. To achieve such goal, initially, we need to estimate the leaving point of probe vehicles, i.e. where and when probe vehicles leave the queue. The estimation of leaving point of probe vehicles is important since the leaving points are ideally supposed to be on the discharging shockwave line. From the formulas of kinematics on one dimension and based on two consecutive data points of a same probe vehicle, which the first one is stopped and the other one is moving (i.e.  $c_i^k = s$ ,  $c_i^{k+1} = m$ , and  $(t_i^k, x_i^k) \in S_j$ ), the time that probe vehicle  $i$  leaves the queue can be calculated as

$$\tau_i^1 = \begin{cases} t_i^{k+1} - \frac{v_i^{k+1}}{2a_{\text{acc}}} - \frac{x_i^{k+1} - x_i^k}{v_i^{k+1}} & \text{if } v_i^{k+1} > \eta * v_{\text{ff}} \\ t_i^{k+1} - \frac{2(x_i^{k+1} - x_i^k)}{v_i^{k+1}} & \text{if } v_i^{k+1} \leq \eta * v_{\text{ff}}. \end{cases} \quad (4a)$$

$$(4b)$$

Equation (4a) corresponds to a vehicle that reaches to its desired speed, which is in a vicinity of the free flow speed, specified by  $\eta \in (0,1)$ . Likewise, (4b) corresponds to a vehicle that its instantaneous speed at time step  $k + 1$  is not its desired speed, since the vehicle is still in the beginning of its trip and accelerating. Note that, there is another possibility that the vehicle has a speed below its desired speed ( $v_i^{k+1} \leq \eta * v_{\text{ff}}$ ) and be in the deceleration stage. In this case, (4b) gives a value less than  $t_i^k$  which is incorrect since,  $\tau_i^1 \in (t_i^k, t_i^{k+1})$ . Therefore, we need to modify (4b) in order to correctly estimate the leaving time of probe vehicle  $i$  that has a speed below the desired speed and is in the deceleration stage. So, if  $v_i^{k+1} \leq \eta * v_{\text{ff}}$  and the  $\tau_i^1$  computed by (4b) is smaller than  $t_i^k$ , the time that probe vehicle  $i$  leaves the queue is

$$\tau_i^1 = t_i^{k+1} - \frac{2(x_i^{k+1} - x_i^k)}{v_i^{k+1}} - \frac{v_{\text{ff}}}{2a_{\text{acc}}} - \frac{x_i^{k+1} - x_i^k}{v_{\text{ff}}} + \frac{(v_i^{k+1} - v_{\text{ff}})^2}{v_{\text{ff}} \cdot a_{\text{dec}}}. \quad (4c)$$

Equation (4c) implies that the vehicle accelerates with acceleration  $a_{\text{acc}}$ , reaches to its desired speed which is equal to  $v_{\text{ff}}$ , and then decelerates with deceleration  $a_{\text{dec}}$  to its speed at time step  $k + 1$ ,  $v_i^{k+1}$ . Ultimately, the leaving point is estimated as  $(\hat{t}_i, \hat{x}_i) = (\tau_i^1, x_i^k)$ . In Fig. 2, filled blue points represent leaving points.

The discharging line has slope  $w$  such that all the moving data of next cycle,  $M_{j+1}$  and stopped data points of the corresponding cycle,  $S_j$  are on its left and right side, respectively. Hence, the estimation of front of queue is formulated as a constrained least square problem:

$$\min_{B_j} J_1 = \sum_{l=1}^{N_L} (\hat{x}_l - w\hat{t}_l - B_j)^2 \quad (5)$$

$$\text{s. t. } \begin{cases} x - wt - B_j \leq \varepsilon_1 & \forall (t, x) \in S_j \\ x - wt - B_j \geq \varepsilon_1 & \forall (t, x) \in M_{j+1}, \end{cases} \quad (6)$$

where  $N_L$  denotes the total number of estimated leaving points and  $B_j$  is the intercept of discharging line shockwave of cycle  $j$ . Note that, given  $B_j$  the start time of green interval of the current cycle denoted by  $t_j^g$  can be calculated as:

$$t_j^g = \frac{x^{\text{max}} - B_j}{w}, \quad (7)$$

where  $x^{\text{max}}$  is the position of intersection stop line from the entrance of the link.

The objective of above problem is to minimize the sum of squared error between the leaving points and the estimated discharging line. Regarding the constraints (6), introduction of  $\varepsilon_1$  provides a tuning parameter to regulate the extent of hardness of the constraints, e.g.  $\varepsilon_1 = 0$  represents hard-constraints that obliges the solution of (5) to fully separate data point of  $S_j$  and  $M_{j+1}$ , whereas a positive value of  $\varepsilon_1$  relaxes the constraints, which is necessary in case of noisy input data, since there might be no line with slope  $w$  that separates noisy data of  $S_j$  and  $M_{j+1}$ . It is worth to mention that, there is no restriction that two consecutive stopped and moving data points ( $c_i^k = s$  and  $c_i^{k+1} = m$ ) to be on the same link. Nevertheless, the chance of finding two such data points in the most downstream link is less comparing to the other links. Thus, in case there is no estimated leaving point (see the first cycle in Fig. 2), the best estimated discharging line in terms of best generalization concept should have the maximum margin from the both stopped ( $S_j$ ) and moving vehicles ( $M_{j+1}$ ). In other words, the discharging line should have the equal distance from the nearest data points of both  $S_j$  and  $M_{j+1}$ . This concept is widely utilized in the support vector machine literature in computer science (Cortes and Vapnik, 1995).

### 3.5 Estimation of the back of queue

The goal of this step is to estimate the manner of queue formation for each cycle ( $j$ ). According to Section II, the back of queue in the  $x$ - $t$  diagram can be modeled by a piecewise linear function comprising several segments that each segment represents a shockwave. Without any explicit information of arrival pattern distribution, the back of queue estimation procedure should determine the number and extent of segments of the piecewise linear function. Initially, similar to the previous step, we need to estimate the joining point of probe vehicles, i.e. where and when probe vehicles join the queue, because the joining points ideally belong to the piecewise linear shockwave. In this step, there are four types of consecutive data points that provide us with the joining points,

- (i) two consecutive data points of probe vehicle  $i$  that the first one is moving and the other one is stopped, i.e.  $(t_i^{k-1}, x_i^{k-1}) \in M_j$  and  $(t_i^k, x_i^k) \in S_j$ ,
- (ii) two consecutive data points of probe vehicle  $i$  that both are stopped, i.e.  $(t_i^{k-1}, x_i^{k-1}) \in S_{j-1}$  and  $(t_i^k, x_i^k) \in S_j$ ,
- (iii) two consecutive data points of probe vehicle  $i$  that both are moving, i.e.  $(t_i^{k-1}, x_i^{k-1}) \in M_j$  and  $(t_i^k, x_i^k) \in M_{j+1}$ ,
- (iv) two consecutive data points of probe vehicle  $i$  that the first one is stopped and the second one is moving, i.e.  $(t_i^{k-1}, x_i^{k-1}) \in S_{j-1}$  and  $(t_i^k, x_i^k) \in M_{j+1}$ .

If the data at time step  $k$  belongs to the  $M_{j+1}$ , this data point can be converted to a queue leaving point according to (4), since the discharging line of the cycle  $j$  is already estimated in the fourth step. Therefore, data points of type (iii) and (iv) can be readily converted to type (i) and (ii), respectively. By using similar equation to (4), the joining point,  $(\check{t}_i, \check{x}_i)$ , can be estimated. In Fig. 2, filled green, yellow, and cyan points respectively represent joining points of type (i), (ii), and (iii). Note that for data type (ii), the leaving point of probe vehicle  $i$  can be estimated by utilizing stopped data  $(t_i^{k-1}, x_i^{k-1})$  and the discharging line of the previous cycle,  $j - 1$ . (The discharging line of the previous cycle is already known, because queue profile estimation advances cycle by cycle in time.) Remarkably, since the first data point of type (ii) is discharging from the queue of the previous cycle, it arrives at capacity state to the

queue of the current cycle that based on LWR theory, obligates the slope of the corresponding segment of back of queue shockwave to be  $w$ .

Given the estimated joining points, the piecewise linear shockwave,  $f_p(x)$ , should be estimated to i) be as close as possible to them, and ii) separate all the moving data associated with the cycle  $j$ ,  $M_j$ , and stopped data points of cycle  $j$ ,  $S_j$  on its left and right side, respectively (see (11)). Further, based on LWR theory, the slope of each segment of the piecewise linear function should be between zero and  $w$  (see (12)). Note that, if a leaving point of type (ii) or (iv) is associated with a segment of  $f_p(x)$ , the segment slope should be equal to  $w$ . To incorporate all the aforementioned physical properties, the estimation of the back of queue with  $N$  piecewise linear segments is formulated as the following nonlinear program:

$$\min_{\substack{\alpha_1, \dots, \alpha_{N-1} \\ \beta_1, \dots, \beta_{N+1}}} J_2 = \sum_{l=1}^{N_j} (\mathcal{D}(f_p(\cdot), (\check{t}_l, \check{x}_l)))^2 + \lambda N \quad (8)$$

$$\text{s. t. } f_p(x) = \begin{cases} \beta_1 + \frac{x-x^{\max}}{\alpha_1-x^{\max}} (\beta_2 - \beta_1) & \alpha_1 < x \leq x^{\max} \\ \vdots \\ \beta_n + \frac{x-\alpha_{n-1}}{\alpha_n-\alpha_{n-1}} (\beta_{n+1} - \beta_n) & \alpha_n < x \leq \alpha_{n-1} \\ \vdots \\ \beta_N + \frac{x-\alpha_{N-1}}{x_j^{\min}-\alpha_{N-1}} (\beta_{N+1} - \beta_N) & x_j^{\min} \leq x \leq \alpha_{N-1} \end{cases} \quad (9)$$

$$x_j^{\min} < \alpha_{N-1} < \dots < \alpha_1 < x^{\max} \quad (10a)$$

$$t_{j-1}^g < \beta_1 < \dots < \beta_{N+1} \leq t_j^c \quad (10b)$$

$$\begin{cases} f_p(x) - t \leq \varepsilon_2 & \forall (t, x) \in S_j \\ f_p(x) - t \geq \varepsilon_2 & \forall (t, x) \in M_j \end{cases} \quad (11)$$

$$\frac{\beta_{n+1}-\beta_n}{\alpha_n-\alpha_{n-1}} \leq \frac{1}{w}; n = 1, \dots, N, \quad (12)$$

where  $N_j$  denotes the total number of estimated joining points,  $\varepsilon_2$  similarly to  $\varepsilon_1$ , regulates the extent of hardness of the constraints (11), and function  $\mathcal{D}$  calculates distance of a point from a piecewise line. Hence the first term of right hand side of problem (8) is to minimize the sum of squared distance between the joining points and the desired piecewise linear function. Given that  $f_p(x)$  comprises of  $N$  segments; (8) optimizes  $2N$  parameters defining slope and extent of segments, i.e.  $\alpha_1, \dots, \alpha_{N-1}$  that are associated with the x-axis extent of segments and  $\beta_1, \dots, \beta_{N+1}$  that are associated with the t-axis extent of segments. It is apparent that as  $N$  increases,  $f_p(x)$  becomes more complex and can attain better optimization results in oppose to higher chance of overfitting. To prevent overfitting, it is needed to balance the number of parameters, as an indicator of complexity, and the value of objective function. This can be done by adding a complexity penalty term to the objective function,  $\lambda N$ , where  $\lambda$  is the regularization parameter. Finally to find the optimum solution of (8), we restrict  $N \leq \sqrt{N_j}$ .

Moreover, (12) ensures  $f_p(x)$  to be connected and be in proper intervals, i.e.  $x_j^{\min} \leq x \leq x^{\max}$  and  $t_{j-1}^g < t \leq t_j^c$ . In other words, (10a) ensures the extent of the back of queue shockwave in x-axis to be between the position of intersection stop line,  $x^{\max}$ , and the

position of the furthest queued vehicle from the intersection for cycle  $j$  (the last position of queue of cycle  $j$ ),  $x_j^{\min}$ . To approximate  $x_j^{\min}$ , the furthest position of available probe information as the most conservative estimator can be utilized. So  $x_j^{\min}$  is the minimum between two values: i) the furthest position from intersection among stopped data  $S_j$  (see cycles 1 and 3 in Fig. 2), and ii) the furthest position among the estimated joining points (see cycles 2 and 4 in Fig. 2). Note that,  $x_j^{\min}$  is the position that the estimated discharging line (Section III-D) and piecewise back of queue shockwave are connected to each other with a horizontal line (slope equals to zeros) to close the queue profile polygon (see Fig. 2). Also (10b) implies that the estimation of start time of red interval of current cycle,  $\beta_1$ , should be after the start time of green interval of previous cycle denoted by  $t_{j-1}^g$ . In addition, the back of queue piecewise shockwave should be always before the discharging front shockwave in the  $x$ - $t$  plane, i.e. the utmost time extent of the piecewise shockwave,  $\beta_{N+1}$ , be less than the estimated time of queue full clearance, which is denoted by

$$t_j^c = \frac{x_j^{\min} - B_j}{w}. \quad (13)$$

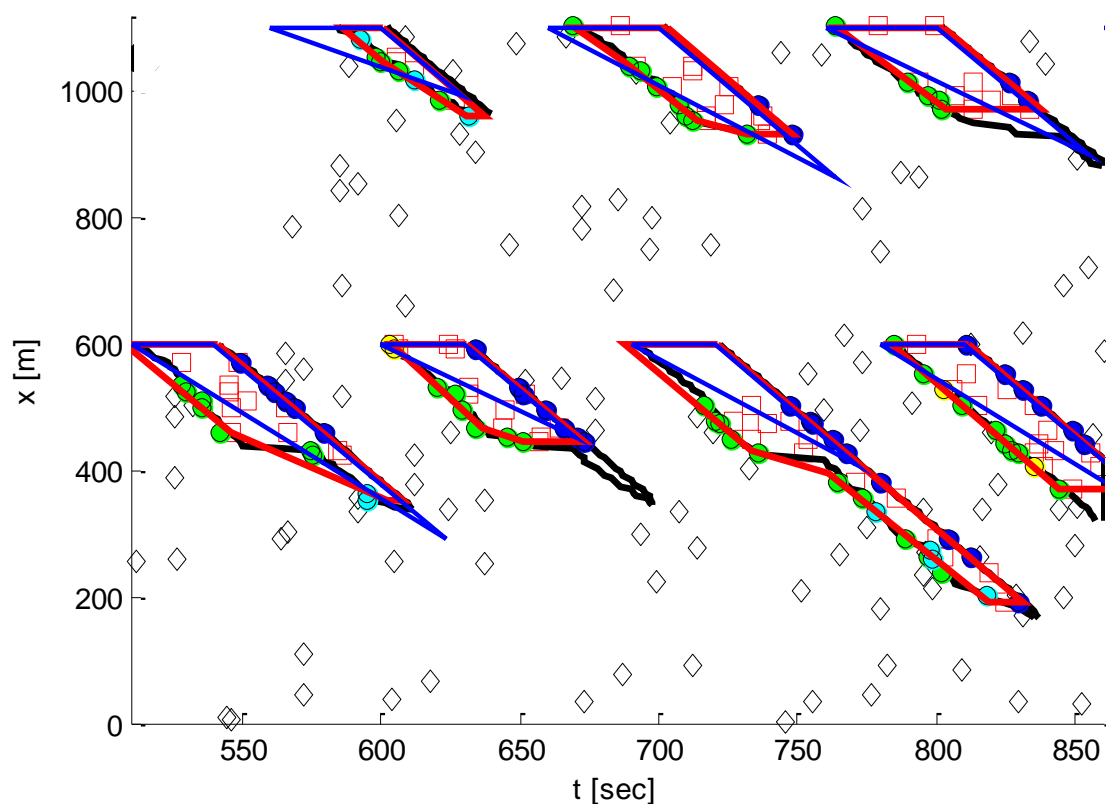
## 4. Results

In this section, the proposed queue profile estimation method is applied to a simulated arterial with two signalized intersections and its outcomes are presented and discussed. We also investigate effect of sampling interval and penetration rate ( $\phi$ ) on the performance of method. Moreover, for further comparison the proposed method is compared with a uniform arrival queue estimation procedure, which requires signal settings data and aggregated data of an upstream (entrance) loop detector. The uniform arrival assumption leads to a triangular queue profile for each cycle (see Fig. 3), where the red interval is one edge, the second edge is discharging shockwave starting at the end of red with slope  $w$ , and the third edge starts from the beginning of red with a slope based on (1), where  $s'$  is the jammed traffic state and state  $s$  is:

$$q_s = \frac{\text{count}_j}{C_j}, k_s = \frac{q_s}{v_{ff}}, \quad (14)$$

where  $C_j$  is the duration of cycle  $j$  and  $\text{count}_j$  is number of vehicles that enter the link and with free flow speed would reach to the intersection stop line during cycle  $j$ .

Figure 3 The ground truth (black) and estimated ( $\phi = 20\%$  and  $T=20$  s) queue profiles based on the proposed method (red), and based on the uniform arrival assumption (blue). Squares and diamonds denote the probe input data.



The simulation with time varying demand lasts for 30 minutes and traffic signals are fixed-time each with different signal settings (that are unknown for the model). In addition, lengths of links are respectively 600 and 500 (m). Conditions of spillbacks are not considered in this analysis, as this is ongoing work. The parameters of the proposed method are chosen as:  $v_{th} = 1 \left(\frac{m}{s}\right)$ ,  $\eta = 0.8$ ,  $a_{acc} = 3 \left(\frac{m}{s^2}\right)$ ,  $a_{dec} = -6 \left(\frac{m}{s^2}\right)$ ,  $\varepsilon_1 = \varepsilon_2 = 0$ , and  $\lambda = 1$ . The estimated queue profiles based on the proposed method ( $\varphi = 20\%$  and  $T = 20$  s) and the uniform arrival assumption procedure along with the ground truth queue profiles are shown in Fig. 3. It is evident that the performance of proposed queue profile estimation method is promising and can capture the fundamental characteristics of queue profiles without any information of arrival distribution and signal settings.

It is noteworthy that from the estimated queue profiles, arrival distribution patterns and signal settings can be readily estimated. For quantitative comparison, queue lengths are derived based on the estimated queue profiles (see Fig. 4) and the mean absolute error (MAE) between the ground truth queue size and the estimated queue size is calculated. Fig. 5 illustrates the effect of various penetration rates ( $\varphi = 5, 10, 20, 30, 50\%$ ) and sampling intervals ( $T = 10, 20, 30, 40$  s) on the MAE performance index of the proposed estimation method. It is apparent in Fig. 5 that even in case of sparse probe data the proposed method yields more accurate results than the uniform arrival estimation. Loop detector data can facilitate the developed methodology in case of small penetration rates (e.g. less than 10%) and improve the accuracy of the model.

Figure 4 The estimated ( $\varphi = 20\%$  and  $T = 20$ s) and ground truth queue length for link 1.

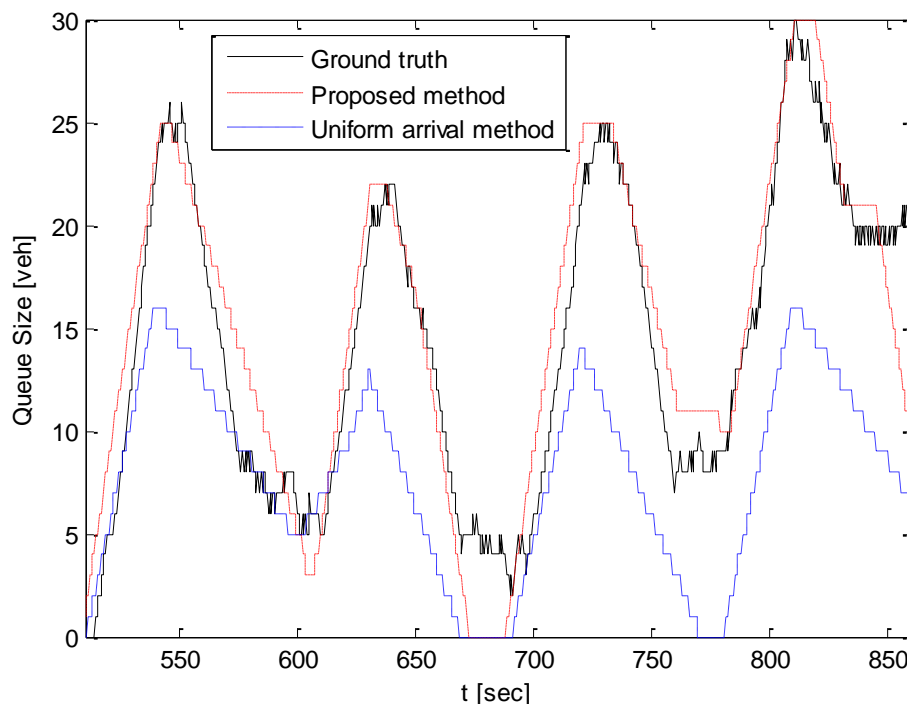
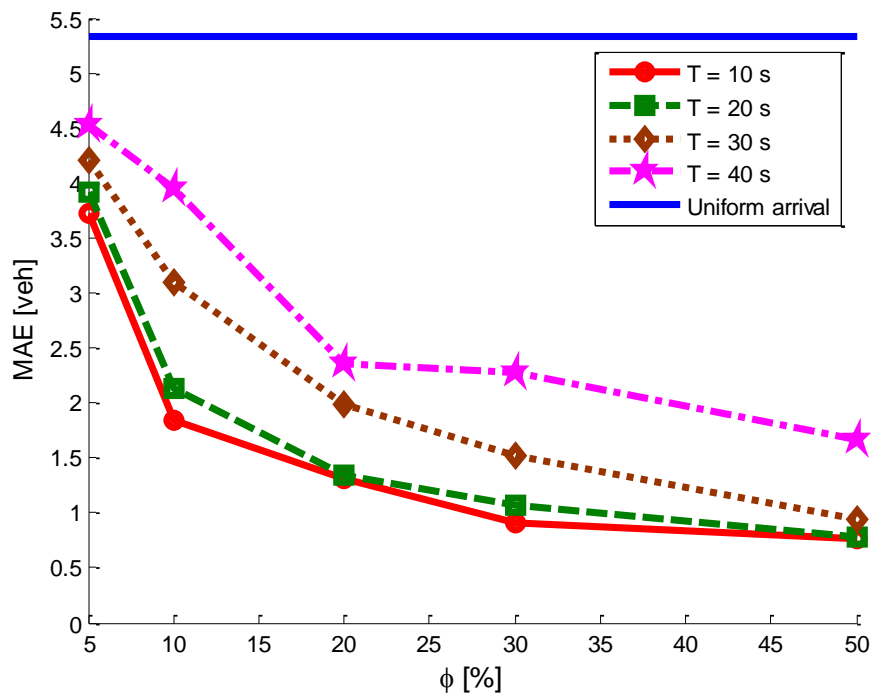


Figure 5 The MAE between the ground truth and estimated queue length with different penetration rates and sampling intervals.



## 5. Conclusion

This paper has presented a method to estimate queue profiles in urban networks, based on LWR traffic theory and leveraging the collective effect of dispersed probe data, which consists of position and velocity of probe vehicles. The significance of proposed method is estimation of shockwaves in signalized intersection without any explicit information of signal settings and arrival distribution. The outcome of proposed method seems promising and more accurate once compared to a uniform arrival queue profile estimation procedure. The effect of penetration rate of probe vehicles and sampling interval on the performance of the method is also studied. The proposed method is beneficial for vehicle trajectory reconstruction, fuel consumption and emission estimation, and travel time allocation problem. Future research will investigate the spillback modeling and further analysis of the method with real traffic data.

## 6. References

- Akçelik, R. (1998) A queue model for HCM 2000, *Technical Note*. ARRB Transport Research Ltd, Vermont South, Australia.
- Ban, X., P. Hao, and Z. Sun (2011) Real time queue length estimation for signalized intersections using travel times from mobile sensors, *Transportation Research Part C*, vol. 19, no. 6, pp. 1133-1156.
- Comert, G. and M. Cetin (2011) Analytical evaluation of the error in queue length estimation at traffic signals from probe vehicle data, *IEEE Transactions on Intelligent Transportation Systems*, vol. 12, no. 2, pp. 563-573.
- Cortes, C. and V. Vapnik (1995) Support-Vector Networks, *Machine Learning*, vol. 20, no. 3, pp. 273-297.
- Darroch, J. N., G. F. Newell, and R. W. J. Morris (1964) Queues for a vehicle-actuated traffic light, *Operations Research*, vol. 12, 882-894, 1964.
- Dion, F., H. Rakha, and Y. Kang (2004) Comparison of delay estimates at under-saturated and over-saturated pre-timed signalized intersections, *Transportation Research Part B*, vol. 38, no. 2, pp. 99-122.
- Geroliminis, N. and A. Skabardonis (2005) Prediction of arrival profiles and queue lengths along signalized arterials by using a markov decision process, *Transportation Research Record*, 1934, pp. 116-124.
- Geroliminis, N. and A. Skabardonis (2011) Identification and analysis of queue spillovers in city street networks, *IEEE Transactions on Intelligent Transportation Systems*, vol. 12, no. 4, pp. 1107-1115.
- Groot, N., B. De Schutter, and H. Hellendoorn (2012) Integrated model predictive traffic and emission control using a piecewise-affine approach, *IEEE Transactions on Intelligent Transportation Systems*, DOI: 10.1109/TITS.2012.2227314.
- Hellinga, B., P. Izadpanah, H. Takada, and L. Fu (2008) Decomposing travel time measured by probe-based traffic monitoring systems to individual road segments, *Transportation Research Part C*, vol. 16, no. 6, pp. 768-782.
- Herrera, J. C., D. B. Work, R. Herring, X. Ban, and A. Bayen (2010) Evaluation of traffic data obtained via GPS-enabled mobile phones: the mobile century field experiment, *Transportation Research Part C*, vol. 18, no. 4, pp. 568-583.
- Hofleitner, A., R. Herring, P. Abbeel, and A. Bayen (2012) Learning the dynamics of arterial traffic from probe data using a dynamic bayesian network, *IEEE Transactions on Intelligent Transportation Systems*, vol. 13, no. 4, pp. 1679-1693.
- Izadpanah, P., B. Hellinga, and L. Fu (2009) Automatic traffic shockwave identification using vehicles' trajectories, in *Proc. 88th Annual Meeting of the Transportation Research Board* (CD-ROM).

- Jelaca, V., J. O. N. Castaneda, A. Pizurica, and W. Philips (2012) Image projection clues for improved real-time vehicle tracking in tunnels, in Proc. *SPIE – The International Society for Optical Engineering*, 8301, art. no. 83010C.
- Kwong, K., R. Kavalier, R. Rajagopal, and P. Varaiya (2009) Arterial travel time estimation based on vehicle re-identification using wireless magnetic sensors, *Transportation Research Part C*, vol. 17, no. 6, pp. 586-606.
- Lighthill, M. J. and G. B. Whitham (1955) On kinematic waves. I: flood movement in long rivers. II: a theory of traffic flow on long crowded roads, *Proceedings of Royal Society (London)* A229, pp. 281-345.
- McNeill, D. R. (1968) A solution to the fixed cycle traffic light problem with compound Poisson arrivals, *Journal of Applied Probability*, vol. 5, no. 3, pp. 624-635.
- Michalopoulos, P. G., G. Stephanopoulos, and G. Stephanopoulos (1981) An application of shock wave theory to traffic signal control, *Transportation Research Part B*, vol.15, no. 1, pp. 31-51.
- Newell, G. F. (1960) Queues for a fixed-cycle traffic light, *The Annals of Mathematical Statistics*, vol. 31, pp. 589-597.
- Newell, G. F. (1965) Approximation methods for queues with application to fixed-cycle traffic light, *SIAM Review* 7, pp. 223-240.
- Ramezani, M. and N. Geroliminis (2012) On the estimation of arterial route travel time distribution with Markov chains, *Transportation Research Part B*, vol. 46, no. 10, pp. 1576-1590.
- Richards, P. J. (1956) Shock waves on the highway, *Operations Research* 4, pp. 42-51.
- Skabardonis, A. and N. Geroliminis (2008) Real-time monitoring and control on signalized arterials, *Journal of Intelligent Transportation Systems*, vol.12, no. 2, pp. 64-74.
- Viti, F. and H. J. van Zuylen (2010) Probabilistic models for queues at fixed control signals, *Transportation Research Part B*, vol. 44, no. 1, pp. 120-135.
- Webster, F. V. (1958) Traffic signal settings, Road Res. Lab. Tech. Paper 39, London, U.K.
- Wu, X. and H. X. Liu (2011) A shockwave profile model for traffic flow on congested urban arterials, *Transportation Research Part B*, vol. 45, no. 10, pp. 1768-1786.
- Wu, X., H. X. Liu, and N. Geroliminis (2011) An empirical analysis on the arterial fundamental diagram, *Transportation Research Part B*, vol. 45, no. 1, pp. 255-266.
- Wu, X., H. X. Liu, and D. Gettman (2010) Identification of oversaturated intersections using high-resolution traffic signal data, *Transportation Research Part C*, vol. 18, no. 4, pp. 626-638.